J Mater Sci (2012) 47:1751–1757
DOI 10.1007/s10853-011-5955-0

The effect of high-pressure torsion on the behaviour of intermetallic particles present in Al–1Mg and Al–3Mg

Jennifer Crump · Xiao Guang Qiao · Marco J. Starink

Received: 15 June 2011 / Accepted: 12 September 2011 / Published online: 28 September 2011

Abstract The effect of severe plastic deformation on intermetallic particles was investigated using high-pressure torsion on an Al–1Mg–0.2Si–0.2Fe–0.3Mn alloy and an Al–3Mg–0.2Si–0.2Fe–0.3Mn (wt%) alloy. Extensive optical microscopy and scanning electron microscopy was performed to analyse the intermetallic particles using image analysis software. It was found that all the intermetallic particles decreased in size with increasing strain whilst their spatial distribution was homogenised. A greater decrease in size was found for the intermetallic particles present in Al–1Mg alloy and the possible causes are discussed. Even though the strain near the centre of the sample is close to zero, refinement of intermetallic particles is substantial at this location.

Introduction

High-pressure torsion (HPT) gives excellent grain refinement and obtains strengthening of metals and alloys [1]. HPT differs from conventional torsion in that it imposes a large hydrostatic pressure of up to several GPa during processing. The HPT sample is a disc, typically with a diameter ranging from 10 to 20 mm and a thickness of about 1 mm [2, 3]. During HPT, the disc-shaped specimen is put into an almost closed die, and a compressing force is imposed on top of the sample. Then, one of the platens is rotated to impose a shear strain in the sample. A large accumulated strain and grain refinement can be achieved through HPT.

J. Crump · X. G. Qiao (✉) · M. J. Starink
Materials Research Group, Engineering Sciences,
University of Southampton, Southampton SO171BJ, UK
e-mail: xgqiao@126.com

Extensive research on severe plastic deformation (SPD) (e.g. on grain refinement [4–6] and hardening [6, 7]) has been performed and in a few studies, refinement of intermetallic particles has been studied [8, 9]. However, to the best of our knowledge no reports are available on the refinement alloys during SPD of Al–Fe–Si–Mn type intermetallic particles typically found in non heat treatable Al–Mg–Mn–Fe type. Intermetallic particles are present in virtually all commercial alloys, and there are two main reasons for this. Firstly, in many cases it is prohibitively expensive to remove all impurities from the master alloys used for casting. Thus, Al alloys will normally always contain some of the main impurities Fe and Si and non soluble intermetallic particles containing 2 or more of the elements Al, Fe and Si, plus any intentional alloying additions [10]. Secondly, non-soluble intermetallic phases can be generated (or modified) because of intentional alloying additions. As a result, virtually all Al-based alloys in commercial use contain intermetallic particles, typically at 1–3 vol% [10–13]. These particles have a range of effects, some positive, some negative. For instance, in most high-strength Al-based alloys intermetallic particles reduce fracture toughness [14, 15] and increase quench sensitivity [16]. In many Al–Mg-based alloys, Fe, Si and Mn are intentionally added to obtain intermetallic particles that are beneficial in controlling microstructure development during thermomechanical processing [17, 18]. Study of particle breakup during SPD is further relevant because of potential application of SPD to recycle type Al-based alloys, which contain substantial amounts of coarse intermetallic particles which need to be refined to enhance applicability of the alloys [19].

With a view to commercialising SPD of light alloys, it is thus important to understand the changes in intermetallic particles induced by the high strains. The large strain and

stress during HPT is expected to enable HPT to break the hard particles in the matrix and to obtain finer particles. Fine and homogenously distributed particles in ultra fine-grained (UFG) materials significantly improve the strength/hardness [20], especially for Al alloys. Remarkable refinement of coarse Si particles of Al–7 wt%Si was achieved through five turns of HPT [21]. Furthermore, stable fine particles can also improve thermal stability of the UFG microstructure through inhibiting grain growth [22].

The fundamental aim of this study is to provide a detailed quantitative analysis on how the intermetallic particles present in Al–Mg-based alloys behave when subjected to HPT. The alloys studied are Al–(1–3)Mg–0.2Si–0.2Fe–0.3Mn alloys, in which α-$Al_{12}(Fe,Mn)_3Si$ and/or Mg_2Si have been identified by thermodynamics simulation and experiments [23, 24]. Extensive optical microscopy and SEM will be performed on samples subjected to varying degrees of HPT.

Experimental

This study was carried out on two Al–Mg-based alloys supplied by Alcan Banbury Laboratory UK; their compositions are shown in Table 1. The alloys will be referred to throughout this article as Al–1Mg and Al–3Mg. The alloys were direct chill (DC) cast, and the ingots were preheated to 540 °C for 4 h followed by hot rolling down to 5 mm. After this, the plates were solution treated at 500 °C for 20 min, quenched, and then cold rolled with a rolling reduction of 60%.

From these alloy sheets, discs of 9.8-mm diameter were machined. The discs were ground and polished to 0.85 mm, and subsequently processed by HPT up to 16 turns at room temperature. During HPT, a pressure of 6 GPa was imposed on the discs, and the anvil was rotated at a speed of 1 rpm. To check for possible sample slippage, we repeated experiments with lines drawn on both side of the sample before HPT. The lines are sharp, clear and on the designed destinations even after 20 turns of HPT, and so there is no sample slippage occurring during the present investigations.

The processed discs were then cold mounted, ground and polished. The intermetallic particles in discs after HPT were observed by an Olympus BH2 optical microscope (OM) and a JEOL JSM 6500F thermal field emission gun scanning electron microscope (FEG-SEM). OM and SEM images were analysed by image processing software ImageJ, and the cross sectional area was chosen as a measure of the size. Measurement was performed on an area of 50 μm × 50 μm. (Note that as a result of this, the average distance to the centre for the measurement performed at the centre will effectively be 14 μm. Whilst the strain in the dead centre is theoretically zero, the average strain experience by the particles in this area will be non-zero.) Particles of size smaller than 0.05 μm^2 were ignored. Both the standard deviation and the standard error of the mean (the standard deviation divided by the square root of the number of particles measured) were calculated. In the figures shown in this article the standard error of the mean is provided.

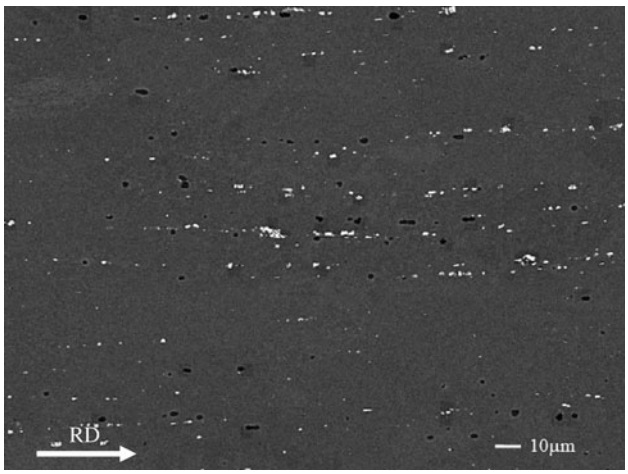

Fig. 1 SEM image of rolled Al–3Mg alloy (i.e. pre-HPT). The particles are aligned in the rolling direction

The hardness of the samples of several HPT samples was tested using a Vickers microhardness tester set at constant load 300 g for 15 s.

Results

The intermetallic particles in as-received condition were stretched along the rolling direction; see Figs. 1 and 2a. After HPT, the particle distribution becomes more homogenous (see, e.g. Fig. 2b).

Table 1 Chemical composition of alloys [23, 24]

Alloy	wt%								
	Mg	Cu	Mn	Fe	Si	Zn	Ti	Cr	B
Al–1Mg	1.02	<0.01	0.25	0.22	0.16	0.003	0.014	0.001	0.0018
Al–3Mg	2.95	<0.01	0.24	0.20	0.15	0.003	0.013	0.001	0.0018

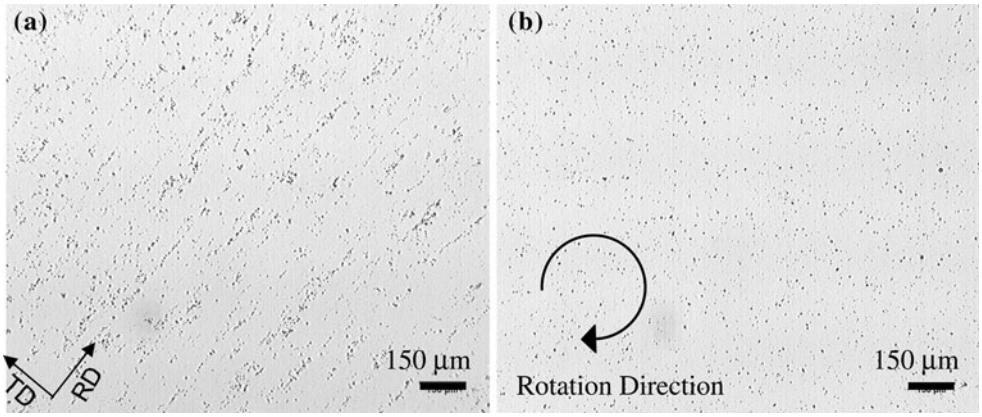

Fig. 2 OM images show particles of Al–3Mg **a** as-received; **b** 16 turns of HPT

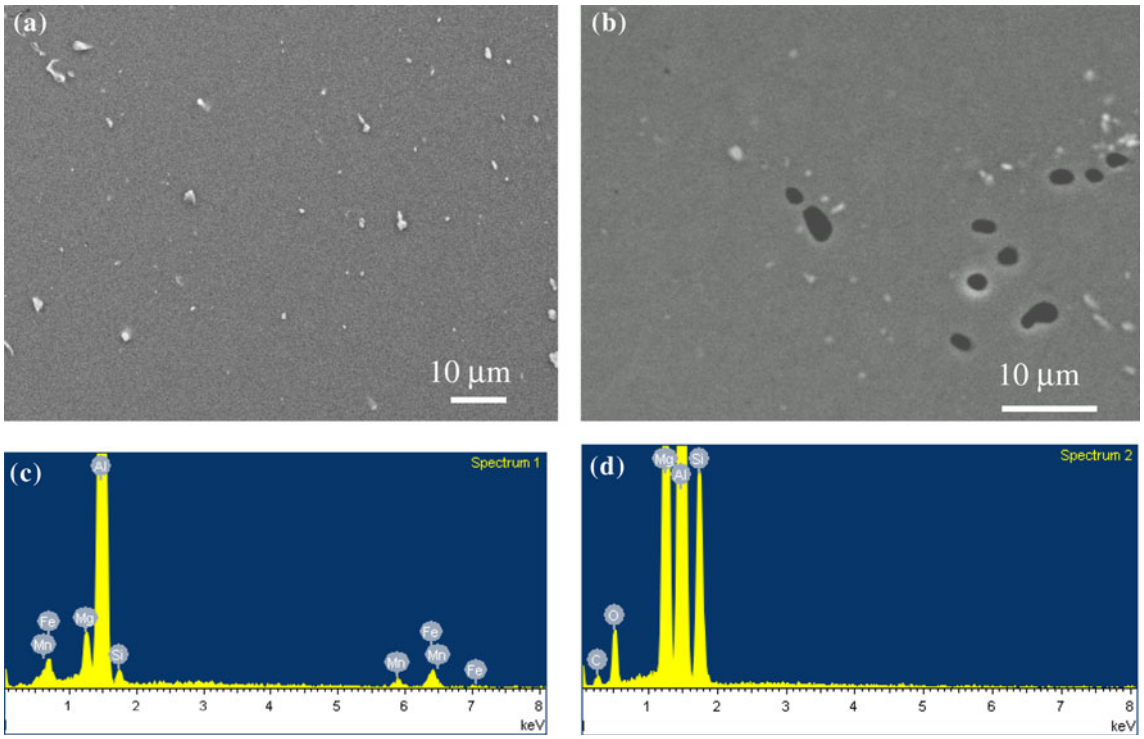

Fig. 3 SEM images of four turns of HPT processed **a** Al–1Mg at edge of sample and **b** Al–3Mg at centre of sample and particles identification by EDS. **c** dark and **d** white particles in (**b**) are identified as α-Al_{12}(Fe,Mn)Si and Mg_2Si, respectively. (Figure 3b is not representative of volume fractions: this micrograph is from an area where a particularly large amount of Mg_2Si was seen.)

Figure 3 shows SEM images of the intermetallic particles of Al–1Mg and Al–3Mg processed by HPT. White particles are observed in both alloys, and EDS analysis (see Fig. 3c) in conjunction with earlier investigations [23, 24] allows for identification of these particles as α-Al_{12}(Fe,Mn)Si. Black particles are observed in Al–3Mg only, and EDS analysis (see Fig. 3d) in conjunction with earlier investigations [23, 24] allows for identification of these particles as Mg_2Si. In a high-magnification SEM image (Fig. 4), a breaking particle is also observed.

Figure 5 shows the measured particle size for the two alloys for samples processed for up to 16 turns by HPT, as measured from OM images. These results show that both Al–1Mg and Al–3Mg show evidence of their intermetallic particles decreasing in size with increasing strain.

Figure 6 shows the average area of intermetallic particles of Al–1Mg and Al–3Mg after various strains by HPT, as measured from OM images. The area measurement was performed on the different positions on the HPT discs from centre to edge. The equivalent strain of each position is calculated through [4, 6, 25, 26].

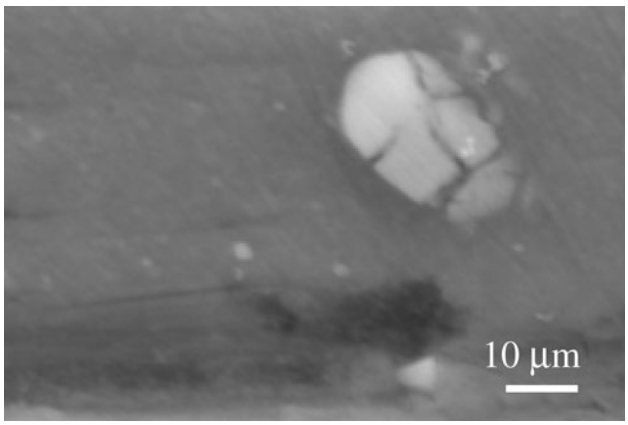

Fig. 4 A breaking particle observed in Al–1Mg processed by 12 turns of HPT

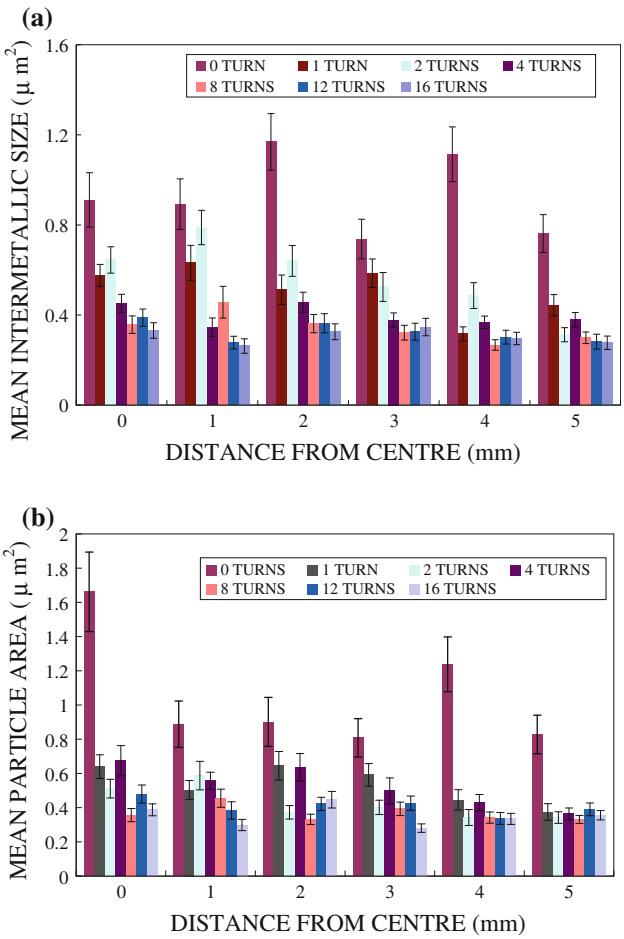

Fig. 5 Measured particle size (mean particle area) for **a** Al–1Mg; and **b** Al–3Mg for samples processed for up to 16 turns by HPT. The particle size shown in (**b**) is average size of α-Al_{12}(Fe,Mn)Si and Mg_2Si

$$\gamma = \frac{2\pi Nr}{h} \tag{1}$$

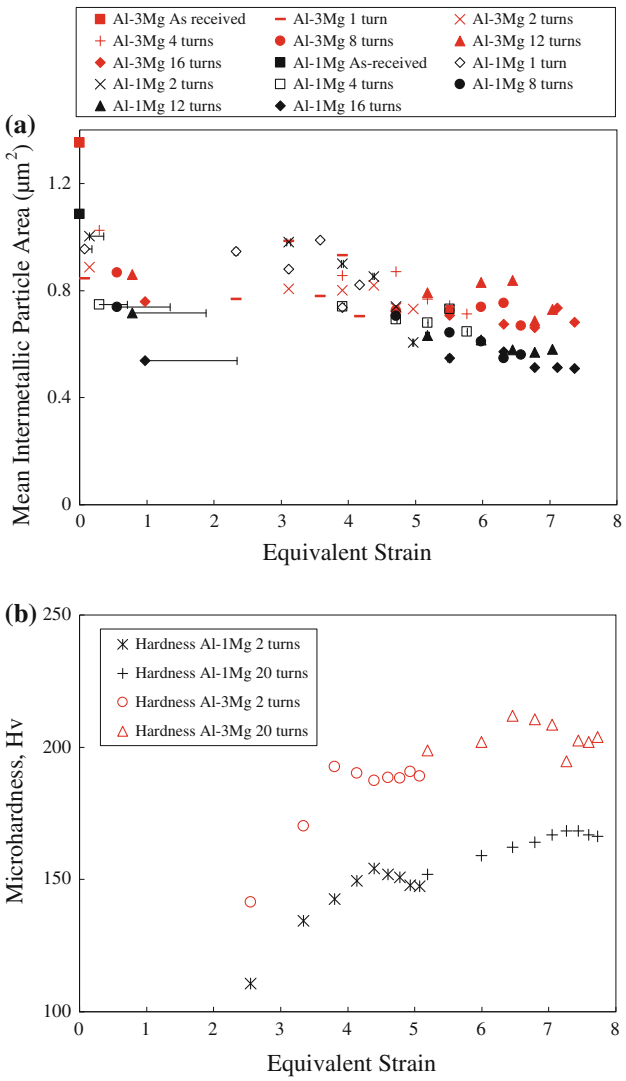

Fig. 6 Dependency of **a** the intermetallic particle size and **b** material hardness on the equivalent strain

$$\varepsilon = \left(\frac{2}{\sqrt{3}}\right) \ln\left[\left(1+\frac{\gamma^2}{4}\right)^{\frac{1}{2}} + \frac{\gamma}{2}\right] \tag{2}$$

where γ is shear strain, N is the number of rotations, r is the distance from the centre of the sample and h is its thickness, and ε is the equivalent strain. The reported strain is the average strain on the 50 μm × 50 μm area over which the particle size is measured.

Figure 6 shows that before HPT, i.e. after rolling, the particles in the Al–3Mg alloy are larger than in the Al–1Mg alloy. After a strain of about 4, the particles of both alloys are refined to a similar size and at strain 7.5 the particles in the Al–3Mg alloy are larger than in the Al–1Mg alloy. The particle size of Al–3Mg remains about constant after strain of 4. It is worth noting that the particle size at the centre of HPT discs, where the equivalent strain is theoretically zero

(see Eqs. 1, 2), is smaller than the particle size of the alloy in as-received condition. Microhardness of Al–1Mg and Al–3Mg are also presented in Fig. 6. Hardness of both alloys increases with increasing equivalent strain, and Al–3Mg is consistently about 40Hv harder than Al–1Mg.

Figure 7 shows the sizes of α-$Al_{12}(Fe,Mn)_3Si$ and Mg_2Si of Al–3Mg at the centre and edge after 4 and 16 turns of HPT. α-$Al_{12}(Fe,Mn)_3Si$ particles are much smaller than Mg_2Si particles. The α-$Al_{12}(Fe,Mn)_3Si$ particle size decreases at both the centre and near the edge of the sample with increasing HPT turn number. However, for the Mg_2Si particle, a significant decrease in size is only observed at the edge after 16 turns of HPT.

Throughout the experiments, no significant changes in the volume fraction of particles with increasing strain were detected.

Discussion

The particles studied in the present study are non-shearable, and unlike the shearable precipitates present in some heat-treatable alloys, they are not prone to dissolution (as observed, e.g. in [27, 28]) on extensive shearing. Owing to low content of Fe and Mn in solution, it is not feasible that α-$Al_{12}(Fe,Mn)Si$ could form because of deformation-induced precipitation such as observed in alloys with higher solute content (see, e.g. [29]). The particles are highly stable, and cannot be dissolved by combinations of hot rolling and solution treatment. These hard non-shearable particles impede dislocation movement during deformation, and the dislocation bypasses the particle by leaving a dislocation loop around it, which is the so-called Orowan bypassing mechanism [30]. With increasing strains, dislocations continuously move to particles and form loops, which cause stress concentration on the particle/matrix interface. The particle breaks when the fracture strength is exceeded. The dislocations also cause hardening of the alloy and grain refinement. Additional transmission electron microscopy analysis (not presented here) confirmed that the HPT processing caused substantial grain refinement in the alloys in line with other reports on similar alloys [1, 2, 5, 31–35]. Vickers microhardness tests confirmed that the alloys experience significant strain hardening during HPT (see Fig. 6). (However, it is to be noted that the refining of the particles should have no direct influence on hardness or strength because they are still too large.)

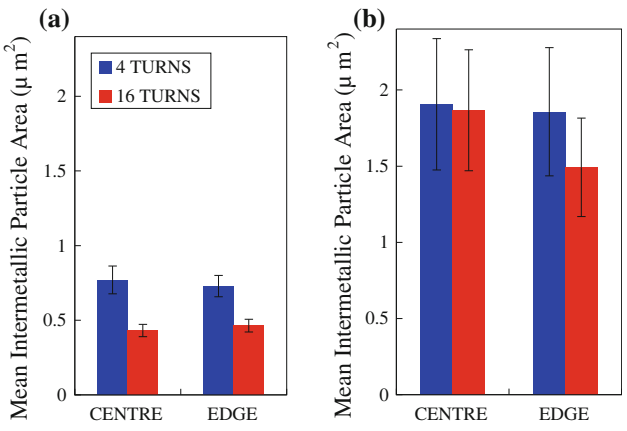

Fig. 7 Effect of HPT turn number on the mean size of intermetallic particles of Al–3Mg measured by SEM. **a** α-$Al_{12}(Fe,Mn)_3Si$, **b** Mg_2Si. *Error bars* represent the standard error of the mean

In the present study, the intermetallic particle sizes of Al–1Mg and Al–3Mg decrease with increasing strain because of the particle breakage (see Fig. 4). However, the rate of particle refinement at strains below 3 is larger in the Al–3Mg alloy as compared with the Al–1Mg alloy (see Fig. 6), and at strains 5–7.5, the particle size of Al–1Mg is smaller than that of Al–3Mg (see Fig. 6). If we just consider continuum mechanics, then the main factors influencing the stresses experienced by each intermetallic particle would be their shape and size and the flow stress of the matrix immediately adjacent to the particle, with higher flow stress causing greater stresses on the particle [36]. Following this, the main reason for the more rapid refinement at strains up to 3 in the Al–3Mg alloy is that the particle size of Al–3Mg in as-received condition is larger than that of Al–1Mg and this causes larger stresses on the particles. However, it is clear that basic continuum mechanics cannot explain the stronger refinement in the Al–1Mg alloy at strains over 4, as the Al–1Mg is the weaker of the two alloys.

Instead, one reason for the limited particle refinement in the Al–3Mg alloy is thought to lie in the stronger grain refinement experienced in this alloy. It has been shown that increased Mg content strongly increases grain refinement during SPD. A recent model of grain refinement [31] (tested against substantially a large database on grain refinement) indicates that at strain 4 the grain size in the Al–3Mg alloy is about 100 nm, and in the Al–1Mg alloy it is about 400 nm. Hence, the Al–3Mg alloy will be much more able to accommodate the macroscopic strain because of the torsion in grain boundaries, and less strain needs to be accommodated by the intermetallic particles.

Also the presence of Mg_2Si particles in the Al–3Mg alloy is thought to have some influence on the evolution of the particle size seen in optical microscopy. Mg_2Si is often used as a reinforcement particle in Mg matrix composites [37] and is a very hard intermetallic (hardness is about 450 kg/mm^2 [38]). Thermodynamic modelling predictions suggest that about 20 vol% of the intermetallic particles in the Al–3Mg alloys is Mg_2Si [24, 39]. The size of Mg_2Si is

much larger than α-$Al_{12}(Fe,Mn)_3Si$ (see Figs. 3b, 7), and it does not decrease very much at HPT turns of the range 4–16 (see Fig. 7b). A small decrease of 15% in size is only observed at edge after 16 turns of HPT (see Fig. 7b). As a result, the mean particle area of Al–3Mg by averaging the size of α-$Al_{12}(Fe,Mn)_3Si$ and Mg_2Si is larger than that of Al–1Mg after larger strains. It is also possible that the Al–rich phase adjacent to the Mg_2Si particle has a reduced Mg content (because of Mg diffusion towards the particle), which causes a local softened layer around the particle, which reduces stresses on it [36].

The particle size measured at the disc centre differs substantially between the samples processed to several turns (see Fig. 6), even though, in theory, the strain would be zero in all cases. The reason for this is thought to lie in the deviations in location of the centre of the disc, which are estimated to be up to 100 μm, which means that the measured particles will in fact have experienced substantial strain of up to 2.3 (16 turns).

Even though the strain near the centre of the sample is close to zero, Fig. 6 shows that refinement of intermetallic particles is substantial at this location. For instance, the particle refinement for the centre of the Al–1Mg alloy at 16 turns (strain $1+^{1.3}_{0.0}$) is similar to that in samples that experienced a strain of about 6. It is thought that this is predominantly due to the strong strain gradient, which causes the generation of geometrically necessary dislocations (GNDs) [6, 35] which will cause additional stresses on the intermetallic particles. For instance, at 25 μm from the centre for a sample processed by 16 turns, the density of GNDs is about 5×10^{14} m^{-2} (see, e.g. [6, 35]), which is similar to the density of statistically stored dislocations generated for $\sim$4 turns at 2 mm from the centre.

Overall, the present results show that whilst HPT is able to further refine the intermetallic particles present in these rolled alloys, the level of refinement is limited. Thus, one has to take into account that for SPD-processed Al alloys, which will have a high strength due to the high dislocation densities and refined grain size, toughness and ductility can be reduced because of these coarse intermetallic particles (see, e.g. [14, 15]).

Conclusions

In this study extensive analysis of the behaviour of intermetallic particles present in Al–1Mg and Al–3Mg subjected to HPT was studied. The following conclusions are drawn:

The intermetallic particles decrease in size for both Al–1Mg and Al–3Mg, whilst the spatial distribution is homogenised.

The average intermetallic particle size at strains greater than 5 is smaller for the Al–1Mg alloy.

The Mg_2Si intermetallic particles are larger in size than the α-$Al_{12}(Fe,Mn)_3Si$ intermetallic particles, but much lower in abundance. It is also suggested that these particles are stronger and require greater dislocation pile-ups to fracture.

Even though the strain near the centre of the sample is close to zero, refinement of intermetallic particles is substantial at this location.

Acknowledgements XGQ gratefully acknowledges the funding support received from the Engineering and Physical Sciences Research Council (EPSRC) PhD plus Grant No. EP/P503841/1. The authors thank Dr Zhihua Zhu and Dr G. Mahon for the rolling of the alloys, and in addition, Dr Zhihua Zhu for performing additional SEM analysis (for Fig. 1). The authors also thank Mr William Vousden for microhardness testing, and Dr Nong Gao for discussion regarding HPT.

References

1. Valiev RZ, Estrin Y, Horita Z, Langdon TG, Zehetbauer MJ, Zhu YT (2006) JOM 58:33
2. Valiev RZ, Alexandrov IV (2002) Ann Chim Sci Mat 27:3
3. Xu C, Horita Z, Langdon TG (2007) Acta Mater 55:203
4. Zhilyaev AP, Nurislamova GV, Kim BK, Baró MD, Szpunar JA, Langdon TG (2003) Acta Mater 51:753
5. Sakai G, Horita Z, Langdon TG (2005) Mater Sci Eng A393:344
6. Zhang J, Starink MJ, Gao N (2011) Mater Sci Eng A 528:2581
7. Kawasaki M, Figueiredo RB, Langdon TG (2011) Acta Mater 59:308
8. Sha G, Wang YB, Liao XZ, Duan ZC, Ringer SP, Langdon TG (2010) Mater Sci Eng A 527:4742
9. Senkov ON, Froes FH, Stolyarov VV, Valiev RZ, Liu J (1998) Scripta Mater 38:1511
10. Wang SC, Starink MJ (2005) Int Mater Rev 50:193
11. Toda H, Kobayashi T, Takahashi A (2000) Mater Sci Eng A 280:69
12. Warmuzek M, Mrowka G, Sieniawski J (2004) J Mater Proc Tech 157–158:624
13. Starink MJ, Wang S (2010) Scripta Mater 62:720
14. Hahn GT, Rosenfield AR (1975) Metall Trans 6A:653
15. Morgeneyer TF, Besson J, Proudhon H, Starink MJ, Sinclair I (2009) Acta Mater 57:3902
16. Liu SD, Zhang XM, Chen MA, You JH (2008) Mater Charact 59:53
17. Johnsson M (1995) Thermochim Acta 256:107
18. Ning JL, Jiang DM (2007) Mater Sci Eng A 452–453:552
19. Szczygiel P, Roven HJ, Reiso O (2005) Mater Sci Eng. A 410–411:261
20. Ashby MF (1971) In: Kelly A, Nicholson RB (eds) Strengthening methods in crystals. Elsevier, Amsterdam, p 137
21. Zhilyaev AP, Garcia-Infanta JM, Carreno F, Langdon TG, Ruano OA (2007) Scripta Mater 57:763
22. Oh-ishi K, Horita Z, Smith DJ, Langdon TG (2001) J Mater Res 16:583
23. Zhu Z, Starink MJ (2008) Mater Sci Eng A489:138
24. Zhu Z, Starink MJ (2008) Mater Sci Eng A488:125
25. Polakowski NH, Ripling EJ (1966) Strength and structure of engineering materials. Prentice-Hall, Englewood Cliffs

26. Valiev RZ, YuV Ivanisenko, Rauch EF, Baudelet B (1996) Acta Mater 44:4705
27. Horita Z, Oh-ishi K, Kaneko K (2006) Sci Techn Adv Mater 7:649
28. Shabashov VA, Korshunov LG, Mukoseev AG, Sagaradze VV, Makarov AV, Pilyugin VP, Novikov SI, Vildanova NF (2003) Mater Sci Eng A 346:196
29. Cepeda-Jimenez CM, Garcia-Infanta JM, Zhilyaev AP, Ruano OA, Carreno F (2011) Mater Sci Eng A 528:7938
30. Orowan E (1934) Z. Physik 89:605, 614, 634
31. Starink MJ, Qiao XG, Zhang J, Gao N (2009) Acta Mater 57:5796
32. Mazilkin AA, Straumal BB, Rabkin E, Baretzky B, Enders S, Protasova SG, Kogtenkova OA, Valiev RZ (2006) Acta Mater 54:3933
33. Lee Z, Zhou F, Valiev RZ, Lavernia EJ, Nutt SR (2004) Scripta Mater 51:209
34. Straumal BB, Baretzky B, Mazilkin AA, Phillipp F, Kogtenkova OA, Volkov MN, Valiev RZ (2004) Acta Mater 52:4469
35. Qiao XG, Gao N, Starink MJ (2011) Phil Mag (in press)
36. Starink MJ (2005) Mater Sci Eng A390:260
37. Gan WM, Wu K, Zheng MY, Wang XJ, Chang H, Brokmeier HG (2009) Mater Sci Eng A 516:283
38. Savitskii EM (1957) Influence of temperature on the mechanical properties of metals and alloys [in Russian], Izd-vo AN SSSR, Moscow, Quoted by Dvorina LA, Popova OI, Derenovskaya NA (1969) Powder Metall Met Ceram 8:363
39. Zhu Z (2006) PhD Thesis, University of Southampton